

See discussions, stats, and author profiles for this publication at: <https://www.researchgate.net/publication/273700158>

Hierarchical Effect Behinds the Supramolecular Chirality of Silver (I)–Cysteine Coordination Polymers.

ARTICLE in THE JOURNAL OF PHYSICAL CHEMISTRY B · MARCH 2015

Impact Factor: 3.3 · DOI: 10.1021/acs.jpcc.5b00847 · Source: PubMed

CITATION

1

READS

60

9 AUTHORS, INCLUDING:



Rosalba Randazzo

University of Catania

8 PUBLICATIONS 82 CITATIONS

SEE PROFILE



Alessandro D'Urso

University of Catania

40 PUBLICATIONS 493 CITATIONS

SEE PROFILE



Giuseppe Compagnini

University of Catania

176 PUBLICATIONS 2,701 CITATIONS

SEE PROFILE



Roberto Purrello

University of Catania

111 PUBLICATIONS 2,923 CITATIONS

SEE PROFILE

Hierarchical Effect behind the Supramolecular Chirality of Silver(I)–Cysteine Coordination Polymers

Rosalba Randazzo,[#] Alessandro Di Mauro,[†] Alessandro D'Urso,^{*,#} Gabriele C. Messina,[#] Giuseppe Compagnini,[#] Valentina Villari,^{‡,§} Norberto Micali,^{‡,§} Roberto Purrello,^{*,#} and Maria Elena Fraga^{*,‡}

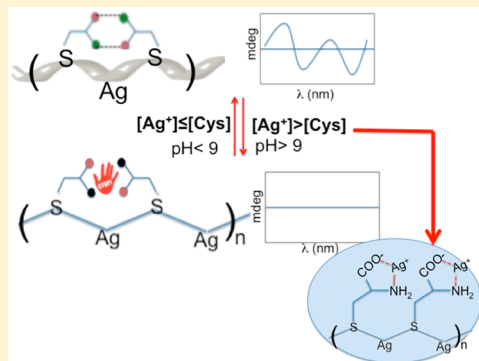
[#]Dipartimento di Scienze Chimiche, and [‡]Dipartimento di Scienze Chimiche and INSTM Udr Catania, Università di Catania, Viale Andrea Doria 6, 95100 Catania, Italy

[†]IMM-CNR, UOS, Via Santa Sofia, 64, 95123 Catania, Italy

[‡]CNR-IPCF Istituto per i Processi Chimico-Fisici Viale F, Stagno d'Alcontres 37, 98158 Messina, Italy

Supporting Information

ABSTRACT: Cysteine is a sulfur-containing amino acid that easily coordinates to soft metal ions and grafts to noble metal surfaces. Recently, chiroptical activity of Ag⁺/cysteine coordination polymers has been widely studied, while, on the other hand, the appearance of a plasmon-enhanced circular dichroic signal (PECD) at the plasmonic spectral region ($\lambda > 400$ nm) has been observed for AgNPs capped with chiral sulfur-containing amino acids. These two events are both potentially exploited for sensing applications. However, the presence of Ag⁺ ions in AgNP colloidal solution deals with the competition of cysteine grafting at the metal NP surface and/or metal ion coordination. Herein we demonstrate that the chiroptical activity observed by adding cysteine to AgNP colloids prepared by pulsed laser ablation in liquids (PLAL) is mainly related to the formation of CD-active Ag⁺/cysteine supramolecular polymers. The strict correlation between supramolecular chirality and hierarchical effects, driven by different chemical environments experienced by cysteine when different titration modalities are used, is pivotal to validate cysteine as a fast and reliable probe to characterize the surface oxidation of AgNPs prepared by pulsed laser ablation in liquids by varying the laser wavelengths.



INTRODUCTION

Interaction of biomolecules with inorganic surfaces has been widely studied, as it represents a straightforward way to modify and trigger material properties for functional application in various fields including sensing, nanomedicine, catalysis, therapy, and many others.¹ Covalent and noncovalent approaches to surface modification can be pursued according to robustness and responsiveness requirements demanded by the applicative context.^{2–5} Recently, the “marriage” between supramolecular and material chemistry has produced original solutions aimed to develop a new class of stimuli-responsive materials, acting both in solution and at the solid surface.

New families of sensors are emerging, whose boosted performances result from combination of specific molecular recognition abilities (based on mastering of weak interactions and dispersive forces) with size-dependent properties of inorganic nanostructures.⁶ In particular, metal nanoparticles are attractive multifunctional materials due to their unique size and chemical and physical properties.^{7–9}

It has been demonstrated that surface plasmon resonance significantly enhances the probing sensitivity.^{10–12} One of the most fascinating aspects of molecular recognition capability based on supramolecular chemistry regards the possibility to

design and develop “smart” systems able to produce a chiral discrimination. Therefore, in recent decades many synthetic approaches have been proposed to fabricate and functionalize the surface of noble metal nanoparticles with chiral molecules or supramolecular complexes to obtain enantioselective sensors, catalysts, or separators.^{13–16} However, integration of chiral sensing systems with rapidly developing nanotechnology and nanomaterials is one of the most challenging requirements for both scientific and technological aspects.^{17,18}

Deprotonated amino acids can chelate/bridge with metal atoms through their amino nitrogen and carboxylate oxygen atoms and form extended helical networks with many metal ions, while if sulfur-containing amino acids are used, SH is mainly involved in the main coordination event. L-Cysteine possesses three functional end groups (SH, COOH, and NH₂) that easily coordinate to soft metal ions (i.e., soft Lewis acids, such as Ag⁺, Hg²⁺, and Cu⁺) and graft to noble metal surfaces.^{19–22}

Received: January 27, 2015

Revised: March 17, 2015



Chiroptical activity of Ag(I)–cysteine (Ag^+/Cys) polymers (in the 230–380 nm spectral region), associated with formation of polymeric species, has been studied in the perspective of development of new sensing systems.²³ On the other hand, the appearance of a plasmon-enhanced circular dichroic signal (PECD), at the plasmonic spectral region ($\lambda > 400$ nm), has been observed for metal NPs capped with a chiral molecule and exploited for sensing applications.^{24,25} These two events have a different origin, since the former is mainly related to the formation of chiral aggregates while the latter is more difficult to be rationalized and its origin is still debatable.^{26,27} Moreover, PECD response of metal NPs is strongly affected by NP dimensions and colloidal solution conditions.

In some cases the CD signal associated with the Ag^+/Cys chiral complex²³ is attributed to interaction of cysteine with AgNPs,^{28–30} despite the clear spectral distinction between the two phenomena. Accordingly, we can reasonably hypothesize that the interference from external factors and “uncontrolled” process conditions strongly impacts the activation of PECD, and consequently not all the AgNP solutions are suitable for such applications.

The aim of this paper is two-fold: first, to elucidate the main factor involved in ligand coordination within AgNP solutions prepared by laser ablation in liquid, and second, to investigate the hierarchical effects dealing with the formation of CD-active species in solution. The present study allows for a clear distinction between cysteine interactions with Ag^0 or Ag^+ species, whose coexistence in AgNP dispersion is often disregarded. In particular, we demonstrate the distinction, even using AgNP colloids obtained by pulsed laser ablation in liquids (PLAL); thus, in the absence of any silver(I) salt, we observe an intense CD signal typical of interaction of Ag^+ ions with cysteine rather than the expected plasma-enhanced CD signal due to grafting of cysteine on the AgNP surface. Among the various approaches used to prepare metal NP colloids, chemical and physical methodologies have been proposed,^{31–39} but the role played by the nanoparticle synthetic procedure on activation of PECD has hardly been discussed. Ag(I) chemical reduction strategies using sodium citrate or NaBH_4 form AgNP colloids having different size distributions, stabilities, and surface compositions, triggered by the reaction conditions. On the other hand, among the physical synthetic approaches that can be used, PLAL of a silver target embedded in water ensures the possibility to obtain colloidal suspensions free of any reaction byproducts or unreacted reagents, with high stability and size control.^{40–43}

Accordingly, we validate the ability of cysteine to work as a chiroptical probe to detect Ag^+ ions in the prepared AgNP colloidal solution, by elucidating, using systematic analytical titrations (using AgNO_3 solutions), the strict correlation between supramolecular chirality Ag^+/Cys complexes and hierarchical effects governing the formation of CD-active species.

EXPERIMENTAL SECTION

AgNPs were prepared by PLAL of a pure silver rod (99.9% Ag by Goodfellow) in ultrapure grade water. The first ($\lambda = 1064$ nm)/second ($\lambda = 532$ nm) harmonic of a Nd:YAG laser with 10 ns pulse width (Surelite II by Continuum) was focused through a convex lens on the target submerged in a vessel filled with the liquid. Ablation was carried out for 15 min at a 10 Hz repetition rate and a fluence of 20 J/cm^2 . The obtained AgNPs had a “naked” surface, since no stabilizer was added, and an

average size of 15–20 nm. Solid AgNO_3 (Sigma-Aldrich) was dissolved in ultrapure water obtained from an Elga Purelab Flex system to obtain a 5 mM aqueous solution.

Citrate-capped AgNPs were prepared by adding 0.5 mL of an aqueous solution of silver nitrate (1%) to an equivalent volume of an aqueous solution of sodium citrate (1%) in 50 mL of boiling ultrapure water. The obtained solution was heated for 20 min and turned from colorless to brown-yellow. After heating, the obtained solution was cooled to room temperature and used after 1:1 dilution in water.³¹ AgNPs are also prepared by chemical reduction using NaBH_4 .³⁸

The stock solutions of L- and D-cysteine were prepared by dissolution of solid cysteine (Sigma-Aldrich) in ultrapure water obtained from an Elga Purelab Flex system by Veolia. Initial cysteine concentration was fixed at 8×10^{-4} M.

UV and CD data were performed with a Jasco V-630 spectrophotometer and a Jasco J-810 spectropolarimeter, respectively, using 1 cm quartz cuvettes. Dynamic light scattering (DLS) experiments were performed by using a He–Ne laser source ($\lambda = 633$ nm) at a power of 35 mW and a Malvern 4700 correlator to analyze the scattered light.⁴⁴ The size distribution of the nanoparticles in solution was obtained by considering that the measured field autocorrelation function, $g_1(Q, t)$, is expressed as the Laplace transform of a continuous distribution $G(\Gamma)$ of decay rates: $g_1(Q, t) = \int G(\Gamma) \exp(-\Gamma t) d\Gamma$, where $Q = (4\pi n/\lambda) \sin(\theta/2)$ is the modulus of the exchanged wave vector, n is the index of refraction of the medium, and θ is the scattering angle. Under the condition $QR \ll 1$ and at high dilution, the decay rate Γ is related to the collective diffusion coefficient at infinite dilution, D_0 , by the relation $\Gamma = D_0 Q^2$.⁴⁵ In turn, D_0 is related to the hydrodynamic radius of the scatterer through the Einstein–Stokes relation: $RH = k_B T / (6\pi\eta D_0)$, where k_B is the Boltzmann’s constant, T is the absolute temperature, and η is the solvent viscosity.

The colloidal separation in solution was carried out by using the asymmetric flow-field fractionation (AF4) method with an AF2000 instrument from Postnova, which allows for fractionating the colloidal solution under hydrodynamic force fields. Due to the different sizes, particles respond to these fields differently, so that smaller particles are transported faster through the channel than the bigger ones. The eluted components, then, flow out of the channel at different times and can be separated.

D/L-Cysteine (5.5×10^{-5} M) was added to 2100 μL of AgNP colloidal dispersion (by fixing absorbance at 0.3 au). Titrations using AgNO_3 as titrant were performed by adding aliquots of AgNO_3 solution (5 mM) to 10 μM L-cysteine. Titrations using cysteine as titrant were performed by adding aliquots of cysteine solution (8×10^{-4} M) to 10 μM AgNO_3 .

RESULTS AND DISCUSSION

AgNP colloidal solutions were prepared by PLAL using both a laser wavelength of 1064 nm (AgNPs@1064) and its second order at 532 nm (AgNPs@532). Addition of L/D-Cys to the AgNPs@532 solution results in a significant variation of the cysteine CD signal (Figure 1). In particular, a bisignate signal (red line for L-Cys and green line for D-Cys) with negative and positive bands centered at 360 and 315 nm, respectively, and a second signal in the Cys region with two negative Cotton effects at 281 and 248 nm and a positive Cotton effect at 209 nm (a mirror image is obtained using D-Cys) are observed. These latter signals are more intense than those observed for free cysteine (red and green dashed lines). No CD signal is

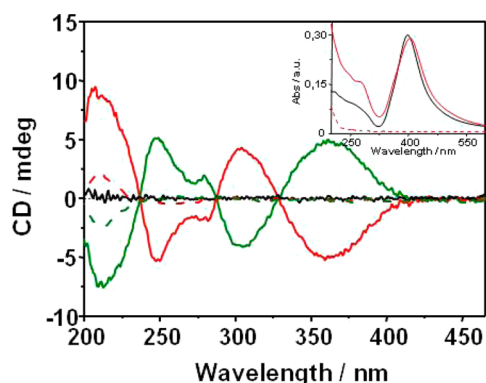


Figure 1. CD and UV spectra of AgNPs before (black line) and after the addition of L-Cys 5.5×10^{-5} M (red line) and D-Cys 5.5×10^{-5} M (green line). Dashed lines in CD and UV graphs show spectra of L- (red) and D- (green) Cys 5.5×10^{-5} M in solution.

observed for a water solution of AgNPs, shown for comparison (black line).

However, the evident mismatch between the spectral region of the observed CD signal (250–380 nm) and the one expected for the PECD signal (>400 nm) (see inset, Figure 1) rules out the plasmonic origin of the observed chiroptical activity. Noteworthy, dynamic light scattering measurements of AgNPs@532 colloidal solutions show the presence of two size families, with an average hydrodynamic radius of 2 and 40 nm (Figure S1, Supporting Information): after colloidal separation in solution by using the asymmetric flow-field fractionation (AFFF) method, only the 40 nm family remains in solution. We demonstrated that it is possible to observe the PECD signal at 400 nm upon addition of L- and D-cysteine to AgNPs@532 solution after AFFF size selection (Figure 2). Further work from our laboratories will be reported in due course.

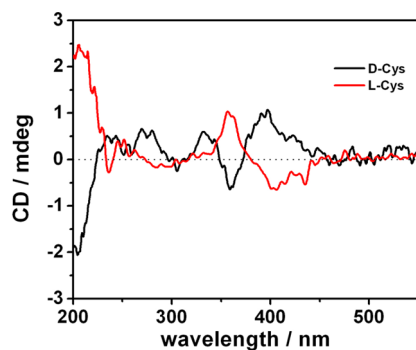


Figure 2. PECD signal of size-separated AgNPs@532 (40 nm) after addition of D-Cys (black line) and L-Cys (red line) solutions.

The observed signal is a clear signature of the binding of cysteine moieties to the silver nanoparticle surface: in fact, by adding L-cysteine or D-cysteine, we get a specular image of the plasmonic band. Although size (and concentration) effects can play a fundamental role in the PECD of metal NP dispersions, we aim to investigate the role played by the presence of Ag^+ ions in pristine solution. To this purpose, we prepared different AgNP colloids using either PLAL or chemical reduction strategies, and we studied their ability to interact with cysteine by following the CD response. To confirm the sensitivity of cysteine to detect the presence of Ag^+ ions in these differently prepared AgNP solutions, we performed CD titrations using

different concentration ranges. We demonstrated that although coordination chemistry allows for prediction of the coordination domains of multitopic ligands toward metal ions, the capability of the obtained compounds to evolve to mono- or multidimensional chains of infinitely extended metal–ligand assemblies in aqueous medium is more complex than expected, as it is affected by hierarchical rules, steric concerns, and system electrostatics.

CD Titrations. AgNO_3 as Titrant. D-Cysteine solution (10 μM , pH 6) was titrated by using aqueous solution of AgNO_3 (5×10^{-3} M), and ECD spectra were recorded after each addition (Figure S2, Supporting Information). No signal is observed if $[\text{Ag}^+] < 2 \mu\text{M}$; this concentration thus represents the sensitivity of the proposed chiral sensor. Above this concentration, a CD signal in the 230–380 nm region is observed, similar in shape to that reported in Figure 1, and assigned to formation of the Ag^+/Cys (M/L) complex.²³ The intensity of the CD signal reaches a maximum value at an M/L ratio of 1:1, as shown in Figure 3. Noteworthy, above the 1:1 (M:L) concentration ratio, the further addition of AgNO_3 causes the progressive decrease of the CD signal.

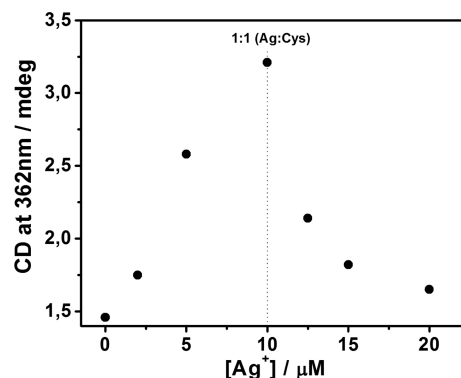


Figure 3. CD signal (@ 362 nm) intensity as a function of the AgNO_3 concentration used as titrant (D-Cys concentration 10 μM).

We confirmed the pH switchable behavior of the observed chiroptical activity both for AgNO_3 /cysteine and for Ag@532 systems (not shown), in good agreement with literature data.²³ Moreover, we observed, for the first time, the detrimental effect of excess Ag^+ on the Ag^+/Cys complex chiroptical activity (Figure 3 and Figure S2, Supporting Information). Since the formation of M_mL_n ($m \neq n$) complexes upon varying the $[\text{Ag}^+]$ and $[\text{Cys}]$ concentrations (due to different coordinative environments with respect to the ML species^{46,47}) cannot be excluded, this result confirms the supramolecular origin of the observed signal, whose CD activity is strictly related to the occurrence of helical structural motifs induced by self-aggregation processes driven by lateral intermolecular interactions. To this regard, it is important to note that Ag^+ is a Lewis acid (while cysteine is not) that can compete with cysteine amino group protonation; in fact, an intramolecular chelation effect fostered by the formation of a five-membered chelation ring between COO^- and NH_2 groups with Ag^+ is responsible for the interruption of intercysteine H-bonds (Figure 4).^{48,49}

By adding/removing the excess Ag^+ , it is possible to switch on/off the CD signal (Figure S3, Supporting Information). This aspect represents a huge limitation in the use of (ML)_n complex formation as a probe to sense cysteine in solution; in

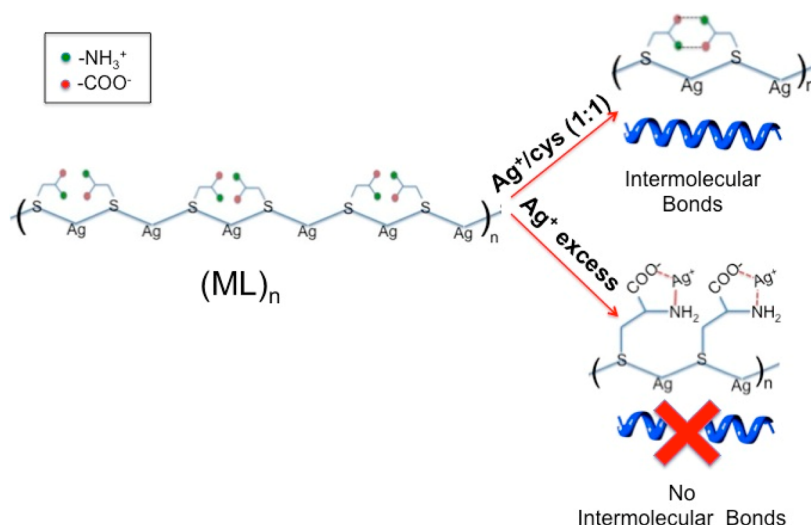


Figure 4. Structural hypothesis of the CD signal (@ 360 nm) on/off switch upon addition of excess AgNO_3 (with respect to 1:1 molar ratio).

fact, if cysteine represents the species whose concentration has to be determined in solution, the addition of an initial excess of silver(I) will produce an analytical “false negative”. Moreover, cysteine solution deterioration needs to be carefully controlled [aqueous solutions of cysteine oxidize readily in air to give cystine at neutral or basic pH (from Sigma-Aldrich/Product Information Sheet)].^{50,51} In fact, by performing a stepwise titration of cysteine solutions (10 μM) obtained from freshly prepared or aged (2 days) concentrated mother solutions (8×10^{-4} M), we observe a shift of the maximum of the CD signal at lower AgNO_3 concentration (Figure S4, Supporting Information). The lower the concentration of cysteine mother solution, the faster the observed degradation. Finally, if we titrate the AgNO_3 solution by slowly adding freshly prepared D-cysteine solution, we do not observe any CD signal at 1:1 ratio; on the contrary, excess cysteine (almost double) seems to be required to reach the maximum CD intensity.

Cysteine as Titrant. AgNO_3 solution (10 μM , pH 6) was titrated by adding an aqueous solution of D-cysteine (8×10^{-4} M), and CD spectra were recorded after each addition (Figure S5, Supporting Information). No signal is observed if $[\text{Cys}] < 10 \mu\text{M}$ (Figure 5), but an M/L concentration ratio of about 1:2 seems to be required to obtain a CD signal having a comparable intensity to that related to the $(\text{ML})_n$ complex recorded in the titration reported in Figure 3. However, as soon as we reach the 1:1 concentration ratio, starting from an initial excess (10 μM)

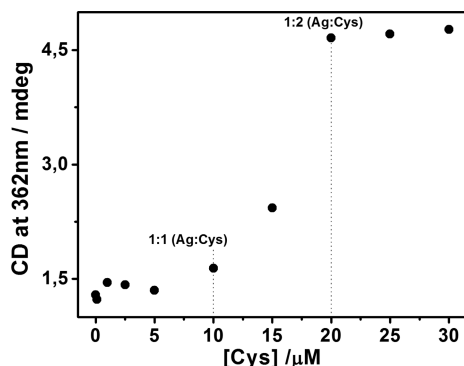


Figure 5. CD signal (@ 362 nm) intensity as a function of the D-Cys concentration used as titrant (AgNO_3 concentration 10 μM).

of AgNO_3 , if we wait for a time frame ranging from a few minutes to 1 h, the expected $(\text{ML})_n$ signal becomes detectable. We can rationalize this result by assuming that, starting from an Ag^+ excess, formation of $(\text{M}_x\text{L}_y)_n$ species ($x > y$), promoted by a multiple coordination of silver ions to cysteine through (i) the thiolate groups (forming $-\text{Ag}-\text{S}-\text{Ag}-\text{S}-$ chains) and (ii) lateral amino acid moieties, can be hypothesized (Figure 6).

Accordingly, the Ag^+ ions are buried within an Ag^+/Cys polymeric structure (Figure 6) whose “secondary structure” lacks lateral interconnection within cysteine chains. In this “random coiled” network, Ag^+ ions are less prone to interact with cysteine and an induction time or an initial addition of higher cysteine concentration (Figure 5) is required to promote the transition from a CD-silent $(\text{M}_x\text{L}_y)_n$ species to the CD-active $(\text{ML})_n$ one.

We conclude that the different chemical environment experienced by cysteine in the two possible titration modalities strongly affects the reaction pathways that govern $(\text{ML})_n$ complex formation. Therefore, the strict correlation between supramolecular chirality and hierarchical effects is herein confirmed.^{52–54} Noteworthy, as soon as the 1:1 $(\text{ML})_n$ complex is restored, the excess cysteine in solution does not affect its CD activity (Figure 5 and Figure S5, Supporting Information), because of its inability to compete with the protonation of amino groups as, on the contrary, the (acid) Ag^+ does.

Sensing Ag^+ in AgNP Dispersion. CD titrations provide evidence of (i) the ability of excess Ag^+ to interfere with the chiroptical activity of $(\text{ML})_n$ polymer and (ii) the fast degradation of aqueous cysteine solution. Accordingly, we can use freshly prepared cysteine to detect the presence of Ag^+ ions in AgNP colloidal solutions prepared by PLA. This aspect is important for a fast and reliable characterization of the surface of AgNPs prepared by laser ablation, free from any additional capping ligand.

In particular, we observed that the AgNP colloidal solution obtained by using a laser wavelength of 1064 nm ($\text{AgNPs}@1064$) showed a faint CD signal in the 230–380 nm region after addition of cysteine. This result is in good agreement with previous studies that demonstrated the effect of laser irradiation wavelength (532 or 1064 nm) on AgNP surface oxidation.^{55,56} In particular, XPS data evidenced that $\text{AgNPs}@1064$ are characterized by an almost “oxide-free” surface, while $\text{AgNPs}@$

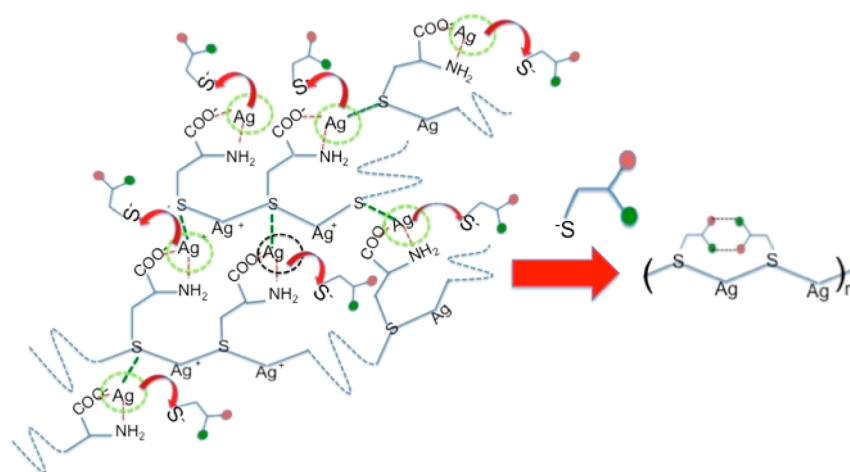


Figure 6. Sketched structure of transition mechanism from $(M_xL_y)_n$ to $(ML)_n$ in the presence of excess cysteine.

532 possess an oxide shell. At this point, we associated the formation of the chiral Ag^+/Cys complex to the ability of oxide at the surface of AgNPs@532 to promote the release of Ag^+ ions in solution (widely investigated for bactericidal activity of silver nanoparticles).⁵⁷ We validated this assumption by comparing the CD signals obtained when cysteine is added to the following solutions: (1) AgNPs@532 (Sol#1); (2) AgNPs@1064 (Sol#2); (3) citrate-capped AgNPs (Sol#3, synthesized using an excess of $AgNO_3$); (4) AgNPs chemically synthesized by reduction of $AgNO_3$ with $NaBH_4$ (Sol#4, synthesized using an excess of $NaBH_4$). Although UV measurements point to AgNP formation for all the investigated synthetic approaches (Figure S6, Supporting Information), not all the solutions are chiroptically active.

CD signals identical in shape (not in intensity) were observed for Sol#1, Sol#2, and Sol#3, while no chiroptical activity was observed for Sol#4 (Figure S7, Supporting Information). In Sol#1 and Sol#3, the observed chiroptical activity can be attributed to the presence of Ag^+ ions in solution that are able to form helical shaped aggregates. The CD intensity detected by adding cysteine to Sol#2 clearly points to an almost negligible $[Ag^+]$ while it is reasonable to assume that Ag^+ ions are almost absent in Sol#4 (as it is obtained using an excess of $NaBH_4$).

Noteworthy, in the AgNP colloidal solution obtained by PLAL it is not possible to predict the Ag^+ concentration, but the presence of these ions strongly influenced the colloidal dispersion properties. Therefore, the evolution of the cysteine CD signal in the 230–380 nm spectral range provides clear evidence of the presence of silver ions whose concentration can be, in this way, quantified. To this purpose, we created a calibration curve, by adding an equimolar quantity of $AgNO_3$ to cysteine solutions having different concentrations (ranging from 1 μM to 100 μM) and by plotting the $(ML)_n$ CD signal intensity (at 362 nm) as a function of the titrant ($AgNO_3$) concentration (Figure 7). Accordingly, the CD signal intensity (at 362 nm) reported in Figure 1 corresponds to an estimated $[Ag^+]$ concentration of about 20 μM in the PLAL-prepared AgNPs@532 solution.

CONCLUSIONS

We have demonstrated the possible use of cysteine solution to detect the presence of Ag^+ ions in AgNP colloidal solutions prepared by pulsed laser ablation in water. The obtained results

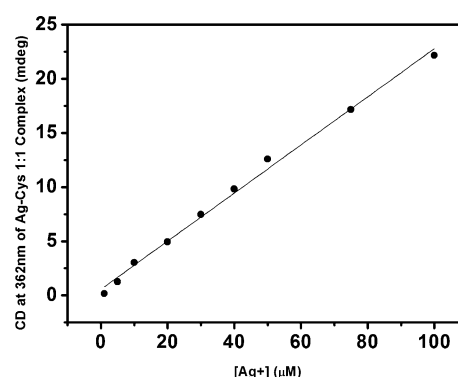


Figure 7. CD signal (@ 362 nm) intensity as a function of equimolar $AgNO_3$ added to D-Cys solutions.

are important for application in water treatment and solar energy conversion strategies.^{58–60} Moreover, we validated the applicability of the Ag^+/Cys chiral system to fully characterize AgNP colloidal solution and define more suitable process conditions to fully exploit the potentialities of PECD, associated with chirality induction to metal NP surfaces. In particular, we shed light on the main factors that play a role in the formation of chiral Ag^+/Cys complexes rather than on the chiral “footprint” of ligand grafting to metallic silver surfaces.

CD titrations elucidated the supramolecular nature of chirality of the Ag^+/Cys aggregates and, even more important, the hierarchical effects that govern the kinetics and evolution of CD-active species. Such aspects, often overlooked, are fundamental to validate the system applicability for sensing. In this context, we evaluated cysteine sensitivity as an indicator of the presence of Ag^+ ions in AgNP colloidal solutions, strongly related to the synthetic approach (chemical or physical) that we used.

As to the use of $AgNO_3$ as a spectroscopic probe to detect cysteine, we have herein demonstrated that excess Ag^+ switches off the CD signal of the formed chiral complex $(ML)_n$ fully restored by further cysteine addition. Finally, working under atmospheric conditions with only freshly prepared cysteine titrant solutions can guarantee a realistic $[Ag^+]$ detection, since less than 1 h after the solution preparation, cysteine deactivation (about 35%) was observed (in addition due to cysteine oxidation to cystine). Thus, the addition of titrant

needs to be carefully defined to avoid the “false negatives” promoted by an unwanted excess of silver ions.

■ ASSOCIATED CONTENT

● Supporting Information

Size distribution of AgNPs obtained by laser ablation before and after the fractionation procedure; CD and UV spectra of AgNO₃/L- or D-Cys solution; CD spectra of Cys-Ag complex with an excess of Ag⁺ before and after the addition of Cys; CD spectra of the Ag/Cys complex using freshly prepared and aged Cys stock solutions; CD and UV spectra of a 10 μM AgNO₃ solution with an increasing amount of L- or D-Cys; UV spectra of AgNP solution, synthesized by different methods; spectra of Cys solution in the presence of AgNPs synthesized by different methods. This material is available free of charge via the Internet at <http://pubs.acs.org>.

■ AUTHOR INFORMATION

Corresponding Authors

*E-mail: me.fragala@unict.it.

*E-mail: adurso@unict.it.

*E-mail: rpurrello@unict.it.

Author Contributions

[§]The manuscript was written through contributions of all authors. All authors have given approval to the final version of the manuscript. V.V. and N.M. contributed equally.

Notes

The authors declare no competing financial interest.

■ ACKNOWLEDGMENTS

The authors thank Ministero dell'Istruzione, dell'Università e della Ricerca Scientifica (MIUR), within project FIRB 2012 RBFR12WB3W.

■ ABBREVIATIONS

PLAL, pulsed laser ablation in liquids; Cys, cysteine; CD, circular dichroism; PECD, plasmon-enhanced circular dichroism; NPs, nanoparticles; DLS, dynamic light scattering; AFFS, asymmetric flow-field fractionation

■ REFERENCES

- (1) Sanchez, C.; Shea, K. J.; Kitagawa, S. Recent Progress in Hybrid Materials Science. *Chem. Soc. Rev.* **2011**, *40*, 471–472.
- (2) D'Urso, A.; Di Mauro, A.; Cunsolo, A.; Purrello, R.; Fragalà, M. E. Solvophobic versus Electrostatic Interactions Drive Spontaneous Adsorption of Porphyrins onto Inorganic Surfaces: A Full Noncovalent Approach. *J. Phys. Chem. C* **2013**, *117*, 17659–17665.
- (3) Smecca, E.; Motta, A.; Fragalà, M. E.; Aleeva, Y.; Condorelli, G. G. Spectroscopic and Theoretical Study of the Grafting Modes of Phosphonic Acids on ZnO Nanorods. *J. Phys. Chem. C* **2013**, *117*, 5364–5372.
- (4) Di Mauro, A.; Mirabella, F.; D'Urso, A.; Randazzo, R.; Purrello, R.; Fragalà, M. E. Spontaneous Deposition of Polylysine on Surfaces: Role of the Secondary Structure To Optimize Noncovalent Coating Strategies. *J. Colloid Interface Sci.* **2015**, *437*, 270–276.
- (5) Pujari, S. P.; Scheres, L.; Marcelis, A. T. M.; Zuilhof, H. Covalent Surface Modification of Oxide Surfaces. *Angew. Chem., Int. Ed.* **2014**, *53*, 6322–6356.
- (6) Wang, S.; Kang, Y.; Wang, L.; Zhang, H.; Wang, Y.; Wang, Y. Organic/Inorganic Hybrid Sensors: A Review. *Sens. Actuators, B* **2013**, *182*, 467–481.
- (7) Edmundson, M. C.; Capeness, M.; Horsfall, L. Exploring The Potential of Metallic Nanoparticles within Synthetic Biology. *New Biotechnol.* **2014**, *31*, 572–578.
- (8) Daniel, M. C.; Astruc, D. Gold Nanoparticles: Assembly, Supramolecular Chemistry, Quantum-Size-Related Properties, and Applications toward Biology, Catalysis, and Nanotechnology. *Chem. Rev.* **2004**, *104*, 293–346.
- (9) Henglein, A. Small-Particle Research: Physicochemical Properties of Extremely Small Colloidal Metal and Semiconductor Particles. *Chem. Rev.* **1989**, *89*, 1861–1873.
- (10) Homola, J.; Yee, S. S.; Gauglitz, G. Surface Plasmon Resonance Sensors: Review. *Sens. Actuators, B* **1999**, *54*, 3–15.
- (11) Bolduc, O. R.; Masson, J. F. Advances in Surface Plasmon Resonance Sensing with Nanoparticles and Thin Films: Nanomaterials, Surface Chemistry, and Hybrid Plasmonic Techniques. *Anal. Chem.* **2011**, *83*, 8057–8062.
- (12) Ben-Moshe, A.; Maoz, B. M.; Govorov, A. O.; Markovich, G. Chirality and Chiroptical Effects in Inorganic Nanocrystal Systems with Plasmon and Exciton Resonances. *Chem. Soc. Rev.* **2013**, *42*, 7028–7041.
- (13) Guerrero-Martínez, A.; Alonso-Gómez, J. L.; Auguie, B.; Cid, M. M.; Liz-Marzán, L. M. From Individual to Collective Chirality in Metal Nanoparticles. *Nano Today* **2011**, *6*, 381–400.
- (14) Barlow, S. M.; Raval, R. Complex Organic Molecules at Surfaces: Bonding, Organisation and Chirality. *Surf. Sci. Rep.* **2003**, *50*, 201–342.
- (15) Nan, J.; Yan, X. P. A Circular Dichroism Probe for L-Cysteine Based on the Self-Assembly of Chiral Complex Nanoparticles. *Chem.—Eur. J.* **2010**, *16*, 423–427.
- (16) Shukla, N.; Bartel, M. A.; Gellman, A. J. Enantioselective Separation on Chiral Au Nanoparticles. *J. Am. Chem. Soc.* **2010**, *132*, 8575–8580.
- (17) Valev, V. K.; Baumberg, J. J.; De Clercq, B.; Braz, N.; Zheng, X.; Osley, E. J.; Vandendriessche, S.; Hojiej, M.; Blejeun, C.; Mertens, J.; et al. Nonlinear Superchiral Meta-Surfaces: Tuning Chirality and Disentangling Non-Reciprocity at the Nanoscale. *Adv. Mater.* **2014**, *26*, 4074–4081.
- (18) Jain, P. K.; Huang, X.; El-Sayed, I. H.; El-Sayed, M. A. Noble Metals on The Nanoscale: Optical and Photothermal Properties and Some Applications in Imaging, Sensing, Biology, and Medicine. *Acc. Chem. Res.* **2008**, *41*, 1578–1586.
- (19) Kathalikkattil, A. C.; Subramanian, P. S.; Suresh, E. Structural Diversity in Two Dimensional Chiral Coordination Polymers Involving 4,4'-Bipyridine and L-Cysteate as Bridging Ligands with Zn and Cd Metal Centres: Synthesis, Characterization and X-Ray Crystallographic Studies. *Inorg. Chim. Acta* **2011**, *365*, 363–370.
- (20) Katagiri, K.; Ikeda, T.; Tominaga, M.; Masu, H.; Azumaya, I. Coordination Polymers and Networks Constructed from Bidentate Ligands Linked with Sulfonamide and Silver(I) Ions. *Cryst. Growth Des.* **2010**, *10*, 2291–2297.
- (21) Katagiri, K.; Sakai, T.; Hishikawa, M.; Masu, H.; Tominaga, M.; Yamaguchi, K.; Azumaya, I. Synthesis, Structure, and Thermal Stability of Silver(I) Coordination Polymers with Bis(pyridyl) Ligands Linked by an Aromatic Sulfonamide: One-Dimensional-Straight Chain, One-Dimensional-Columnar with Helical Components, and Two-Dimensional-Layer Network Structure. *Cryst. Growth Des.* **2014**, *14*, 199–206.
- (22) Du, L. Y.; Shi, W. J.; Hou, L.; Wang, Y. Y.; Shi, Q. Z.; Zhu, Z. Solvent or Temperature Induced Diverse Coordination Polymers of Silver(I) Sulfate and Bipyrazole Systems: Syntheses, Crystal Structures, Luminescence, and Sorption Properties. *Inorg. Chem.* **2013**, *52*, 14018–14027.
- (23) Shen, J. S.; Li, D. H.; Zhang, M. B.; Zhou, J.; Zhang, H.; Jiang, Y. B. Metal–Metal-Interaction-Facilitated Coordination Polymer as a Sensing Ensemble: A Case Study for Cysteine Sensing. *Langmuir* **2011**, *27*, 481–486.
- (24) Lieberman, I.; Shemer, G.; Fried, T.; Kosower, E. M.; Markovich, G. Plasmon-Resonance-Enhanced Absorption and Circular Dichroism. *Angew. Chem., Int. Ed.* **2008**, *47*, 4855–4857.
- (25) Lorenzo, M. O.; Baddeley, C. J.; Muryn, C.; Raval, R. Extended Surface Chirality from Supramolecular Assemblies of Adsorbed Chiral Molecules. *Nature* **2000**, *404*, 376–379.

- (26) Humblot, V.; Haq, S.; Muryn, C.; Hofer, W. A.; Raval, R. From Local Adsorption Stresses to Chiral Surfaces: (*R,R*)-Tartaric Acid on Ni(110). *J. Am. Chem. Soc.* **2002**, *124*, 503–510.
- (27) Gautier, C.; Bürgi, T. Chiral Inversion of Gold Nanoparticles. *J. Am. Chem. Soc.* **2008**, *130*, 7077–7084.
- (28) Li, T.; Park, H. G.; Lee, H. S.; Cho, S. H. Circular Dichroism Study of Chiral Biomolecules Conjugated with Silver. *Nanotechnology* **2004**, *15*, S660–S663.
- (29) Choi, S. H.; Lee, S. H.; Hwang, Y. M.; Lee, K. P.; Kang, H. D. Interaction Between the Surface of the Silver Nanoparticles Prepared by Γ -Irradiation and Organic Molecules Containing Thiol Group. *Radiat. Phys. Chem.* **2003**, *67*, 517–521.
- (30) Rezanka, P.; Záruba, K.; Král, V. Supramolecular Chirality of Cysteine Modified Silver Nanoparticles. *Colloids Surf., A* **2011**, *374*, 77.
- (31) Matijevic, E. Preparation and Properties of Uniform Size Colloids. *Chem. Mater.* **1993**, *5*, 412–426.
- (32) Nickel, U.; Castell, A. Z.; Poppl, K.; Schneider, S. A Silver Colloid Produced by Reduction with Hydrazine as Support for Highly Sensitive Surface-Enhanced Raman Spectroscopy. *Langmuir* **2000**, *16*, 9087–9091.
- (33) Leopold, N.; Lendl, B. A New Method for Fast Preparation of Highly Surface-Enhanced Raman Scattering (SERS) Active Silver Colloids at Room Temperature by Reduction of Silver Nitrate with Hydroxylamine Hydrochloride. *J. Phys. Chem. B* **2003**, *107*, 5723–5727.
- (34) Khanna, P. K.; Subbarao, V. V. S. Nanosized Silver Powder via Reduction of Silver Nitrate by Sodium Formaldehydesulfoxylate in Acidic pH Medium. *Mater. Lett.* **2003**, *57*, 2242–2245.
- (35) I. Sondi, I.; Goia, D. V.; Matijevic, E. J. Preparation of Highly Concentrated Stable Dispersions of Uniform Silver Nanoparticles. *J. Colloid Interface Sci.* **2003**, *260*, 75–81.
- (36) Gutiérrez, M.; Henglein, A. Formation of Colloidal Silver by “Push-Pull” Reduction of Silver(I). *J. Phys. Chem.* **1993**, *97*, 11368–11370.
- (37) Ershov, B. G.; Janata, E.; Henglein, A. Growth of Silver Particles in Aqueous Solution: Long-Lived “Magic” Clusters and Ionic Strength Effects. *J. Phys. Chem.* **1993**, *97*, 339–343.
- (38) Shirtcliffe, N.; Nickel, U.; Schneider, S. Reproducible Preparation of Silver Sols with Small Particle Size Using Borohydride Reduction: For Use as Nuclei for Preparation of Larger Particles. *J. Colloid Interface Sci.* **1999**, *211*, 122–129.
- (39) Solomon, S. D.; Bahadory, M.; Jeyarajasingam, A. V.; Rutkowsky, S. A.; Boritz, C.; Mulfinger, L. Synthesis and Study of Silver Nanoparticles. *J. Chem. Educ.* **2007**, *84*/2, 322–325.
- (40) Compagnini, G.; Messina, E.; Puglisi, O. Spectroscopic Evidence of a Core–Shell Structure in the Earlier Formation Stages of Au–Ag Nanoparticles by Pulsed Laser Ablation in Water. *Chem. Phys. Lett.* **2008**, *457*, 386–390.
- (41) Messina, E.; Compagnini, G.; D’Urso, L.; Puglisi, O.; Bagiante, S.; Scalese, S. Size Distribution and Particle Shape in Silver Colloids Prepared by Laser Ablation in Water. *Radiat. Eff. Defects Solids* **2010**, *165*, 579–583.
- (42) Messina, G. C.; Wagener, P.; Streubel, R.; De Giacomo, A.; Santagata, A.; Compagnini, G.; Barcikowski, S. Pulsed Laser Ablation of a Continuously-Fed Wire in Liquid Flow for High-Yield Production of Silver Nanoparticles. *Phys. Chem. Chem. Phys.* **2013**, *15*, 3093–3098.
- (43) Amendola, V.; Meneghetti, M. Laser Ablation Synthesis in Solution and Size Manipulation of Noble Metal Nanoparticles. *Phys. Chem. Chem. Phys.* **2009**, *11*, 3805–3821.
- (44) Villari, V.; Micali, N. Light Scattering as Spectroscopic Tool for the Study of Disperse Systems Useful in Pharmaceutical Sciences. *J. Pharm. Sci.* **2008**, *97*, 1703–1730.
- (45) Berne, B. J.; Pecora, R. *Dynamic Light Scattering*; Wiley-Interscience: New York, 1976; pp 1–376.
- (46) Andersson, L. O. Study of Some Silver-Thiol Complexes and Polymers: Stoichiometry and Optical Effects. *J. Polym. Sci. Part A-1: Polym. Chem.* **1972**, *10*, 1963–1973.
- (47) Leung, B. O.; Jalilvand, F.; Mah, V.; Parvez, M.; Wu, Q. Silver(I) Complex Formation with Cysteine, Penicillamine, and Glutathione. *Inorg. Chem.* **2013**, *52*, 4593–4602.
- (48) Hancock, R. D. The Basis of Selectivity for Metal Ions in Open-Chain Ligands and Macrocycles. *J. Chem. Educ.* **1992**, *69*, 615–621.
- (49) Li, H.; Siu, K. W. M.; Guevremont, R.; Le Blanct, J. C. Y. Complexes of Silver(I) with Peptides and Proteins as Produced in Electrospray Mass Spectrometry. *J. Am. Soc. Mass Spectrom.* **1997**, *8*, 781–792.
- (50) Routh, J. H. The Decomposition of Cysteine in Aqueous Solution. *J. Biol. Chem.* **1939**, *130*, 297–304.
- (51) Kolthoff, I. M.; Stricks, D. W. Argentometric Amperometric Titration of Cysteine and Cystine. *J. Am. Chem. Soc.* **1950**, *72*, 1952–1958.
- (52) De Napoli, M.; Nardis, S.; Paolesse, R.; Graç, M.; Vicente, H.; Lauceri, R.; Purrello, R. Hierarchical Porphyrin Self-Assembly in Aqueous Solution. *J. Am. Chem. Soc.* **2004**, *126*, 5934–5935.
- (53) Destoop, I.; Xu, H.; Oliveras-Gonzalez, C.; Ghijssens, E.; Amabilino, D. B.; De Feyter, S. “Sergeants-And-Corporals” Principle In Chiral Induction at an Interface. *Chem. Commun.* **2013**, *49*, 7477–7479.
- (54) D’Urso, A.; Fragalà, M. E.; Purrello, R. From Self-Assembly To Noncovalent Synthesis of Programmable Porphyrins’ Arrays in Aqueous Solution. *Chem. Commun.* **2012**, *48*, 8165–8176.
- (55) Compagnini, G.; Messina, G. C.; D’Urso, L.; Messina, E.; Sinatra, M. G.; Puglisi, O.; Zimbone, M. Aggregation Phenomena and Electromagnetic Amplification Properties in Silver Nanoparticles Joined Through Highly Conjugated Carbon Chains. *Open Surf. Sci. J.* **2011**, *3*, 50–54.
- (56) Yan, Z.; Compagnini, G.; Chrisey, D. B. Generation of AgCl Cubes by Excimer Laser Ablation of Bulk Ag in Aqueous NaCl Solutions. *J. Phys. Chem. C* **2011**, *115*, 5058–5062.
- (57) Xiu, Z. M.; Zhang, Q. B.; Puppala, H. L.; Colvin, V. L.; Alvare, P. J. J. Negligible Particle-Specific Antibacterial Activity of Silver Nanoparticles. *Nano Lett.* **2012**, *12*, 4271–4275.
- (58) An, C. H.; Peng, S. N.; Sun, Y. G. Facile Synthesis of Sunlight-Driven AgCl:Ag Plasmonic Nanophotocatalyst. *Adv. Mater.* **2010**, *22*, 2570–2574.
- (59) Li, Y. Y.; Ding, Y. Porous AgCl/Ag Nanocomposites with Enhanced Visible Light Photocatalytic Properties. *J. Phys. Chem. C* **2010**, *114*, 3175–3179.
- (60) Wang, P.; Huang, B. B.; Lou, Z. Z.; Zhang, X. Y.; Qin, X. Y.; Dai, Y.; Zheng, Z. K.; Wang, X. N. Synthesis of Highly Efficient Ag@AgCl Plasmonic Photocatalysts with Various Structures. *Chem. Eur. J.* **2010**, *16*, 538–544.